Quality grading of painted slates using texture analysis

Ovidiu Ghita*, Paul F. Whelan, Tim Carew and Padmapriya Nammalwar

Vision Systems Group, School of Electronic Engineering
Dublin City University, Dublin 9, Ireland

Abstract

This paper details the development of an automated vision-based solution for identification of paint and substrate defects on painted slates. The developed vision system consists of two major components. The first component of the system addresses issues including the mechanical implementation and interfacing the inspection system with the sensing and optical equipment. The second component involves the development of an image processing algorithm that is able to identify the visual defects present on the slate surface. The process of imaging the slate proved to be very challenging as the slate surface is darkly coloured and presents depth non-uniformities. Hence, a key issue for this inspection system was to devise an adequate illumination system that was able to accommodate challenges including the slates' surface depth non-uniformities and vibrations generated by the conveying system. The visual defects are detected using a novel texture analysis solution where the greyscale (tonal characteristics) and texture information are embedded in a composite model. The developed inspection system was tested for robustness and experimental results are presented.

Keywords: On-line inspection system, slate, visual defects, illumination set-up, industrial conveyor, texture analysis.

1. Introduction

Although slate manufacturing is a highly automated process, currently the slates are inspected manually by a human operator who grades them visually as they emerge via a conveyor from the paint process line. The human inspection is dull and monotonous work and this task offers only satisfactory results when applied to high-speed production lines [20]. Thus, our aim was to develop an automated vision-based inspection system (for a review of the system engineering issues in industrial inspection the reader can refer to Batchelor and Waltz [3] and Newman and Jain [13]) that is able to classify the slates for quality so that defective units may be rejected and to gather statistics on the efficiency of the production process.

The authors found no prior relevant work on the automated inspection of painted slates although there is an abundance of references on the subject of ceramic tiles inspection [1,2,6,7,8,17,19]. Though the manufacturing process for ceramic slates and slates are significantly different [4,6], the ceramic tiles are not dissimilar to slates as both products have textured surfaces, have rectangular shapes and the conveying requirements are similar.

All work in the field of ceramics inspection reviewed, used different imaging sub-systems and processing techniques to detect the visual defects present on the surface of the product. The literature review also indicated that of equal importance to the image processing procedure that is employed to quality grade the product, is the adoption of an opto-mechanical solution

* Corresponding author. Tel.: +353-1-7007637; Fax: +353-1-7005508; E-mail: ghitao@eeng.dcu.ie

that minimises spatial and temporal illumination variations. The ceramic inspection systems examined use either diffuse [2,17] or collimated lighting techniques [1]. Line scan cameras are invariably used in an effort to reduce spatial image acquisition non-uniformities. This is motivated by the fact that it is easier to control the light intensity uniformity of a long narrow light stripe than that of a large two-dimensional area [3,13].

The second major component of the vision-based inspection systems is represented by the image processing procedure that is applied in order to detect the visual defects on the surface of the inspected product. The inspection systems reviewed attempted to identify the defects by either applying morphological techniques [2,12,14,16,21] or inspection solutions based on texture analysis [1,9,10,11,17,19]. In this regard, Boukouvalas et al [2] used 1-D convolvers to identify the spot and line defects present on textured ceramic tiles. The convolution masks implemented using the 1-D convolvers can detect defects with widths within a factor of 1.5 of the feature for which the filter is designed. This solution is not applicable to slate inspection as the typical defects present on the slates surface have a large range of sizes. Later, Boukouvalas et al [1] implemented an inspection algorithm based on Wigner distributions that was successfully applied to the inspection of coloured and heavily textured ceramic tiles. This method is more applicable to inspection of highly textured surfaces with repetitive patterns, thus this method is not suitable for slate inspection. Peñarada et al [17] developed an inspection system that used local grey-level intensity histograms to discriminate between acceptable and defective image regions. Although this method appeared to be promising, it proved to be unreliable when applied to slate inspection. This was motivated by the fact that the local greyscale distributions vary widely across different regions of the slate and from slate-to-slate.

Other related implementations include the application of the grey level difference [20], morphological methods [12,14] and texture-based methods [11,18]. These methods proved to be limited to their application as they were not able to produce effective discriminative features that are able to identify robustly the visual defects present on the slate surface.

To devise a robust algorithm for slate inspection proved to be a very challenging task as the slate's surface greyscale information has a heterogeneous distribution and varies from slate-to-slate. To this end, we have devised a novel highly adaptive texture analysis algorithm that is able to accommodate the local variations in the greyscale distribution but at the same time robustly identify the visual defects. Key to its success was the tonal-texture image descriptor that can adaptively balance the tonal characteristics and the texture information.

This paper is organised as follows. Section 2 describes the typical slate defects. Section 3 details the development of the prototype inspection system. Section 4 describes the development of the texture analysis inspection algorithm. Section 5 discusses the experimental results and Section 6 concludes this paper.

2. Description of slate defects

The slates are roofing materials that are painted on a high-speed paint line and are manually inspected when they emerge from a paint line via an industrial conveyor. The human inspector removes the slates that do not meet the inspection criteria.

The slates have a rectangular shape and their top surface is painted in dark grey with a high gloss finish. The defects present on the slate surface can be roughly classed into substrate and paint defects. Paint defects include no paint, insufficient paint, paint droplets, efflorescence paint debris and orange peel. Substrate defects include incomplete slate formation, lumps, depressions and template marks.

Defect type	Defect Size	Description
Insufficient paint	20mm to all area	Reduced gloss level
Missing paint	2mm to all area	Paint missing from some areas
Droplet	2mm to 15mm	Excess dried and cracked paint
Effloresence	5mm to all area	Contaminant preventing correct adherence of paint
Paint dust	2mm to 50 mm	Dried dust on surface
Burn mark	20 mm to all area	Reduce gloss due to overheating
Barring	20mm to all area	Shade variation caused by uneven heating
Spots	1mm to 5mm	Localised shade variation
Shade variation	20mm to all area	Incorrect pre-heating of slate
Template marks	20mm to all area	Substrate defects due to incorrect slate formation/drying
Lumps and depressions	5mm to 100 mm	Substrate defects

Table 1. Description of paint and substrate defects. Note that the size of defects is measured with respect to the cross and moving direction of travel for slate.

The substrate and paint defects may have arbitrary shapes and their size range from one square mm to hundreds of square millimetres (see Table 1). A number of representative paint and substrate defects are illustrated in Figure 1.

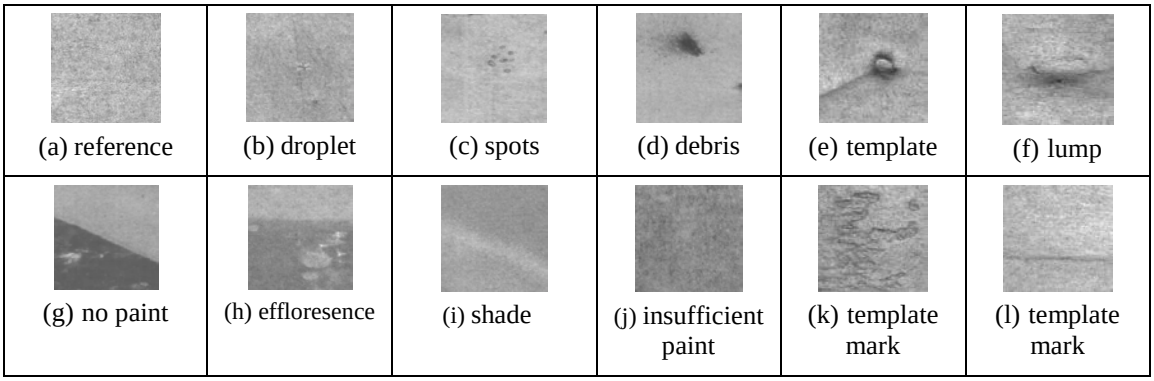

Figure 1. Representative defects found on the slate surface. (a) Defect free slate section. (b-l) Defective slate section.

3 Overview of the developed inspection system

The devised inspection system was built to replicate the factory conditions. Its main components are the opto-mechanical component and the PC which is the host of the inspection software. The opto-mechanical component comprises a two metre long industrial conveyor [Noreside Conveyors and Elevators (Ireland)] and the optical and sensing equipment. The conveyor is able to transport the slate to the inspection line at speeds in the range of 15 to 50 m/min. The sensing equipment consists of a Basler 2k-pixel line–scan camera which is fitted with a 28 mm machine vision lens. The line-scan camera was mounted on a 3 degree of freedom micro-positioner in order to facilitate fine adjustments of camera view line. A Euresys frame grabber assures the interface between the digital line-scan camera and PC. In order to prevent slate rotations when the slate is transported to the inspection line, the slate is aligned by a guide placed on one side of the conveyor and an optical proximity sensor triggers the image capture prior to the arrival of the slate at the inspection line. The prototype inspection system is illustrated in Figure 2.

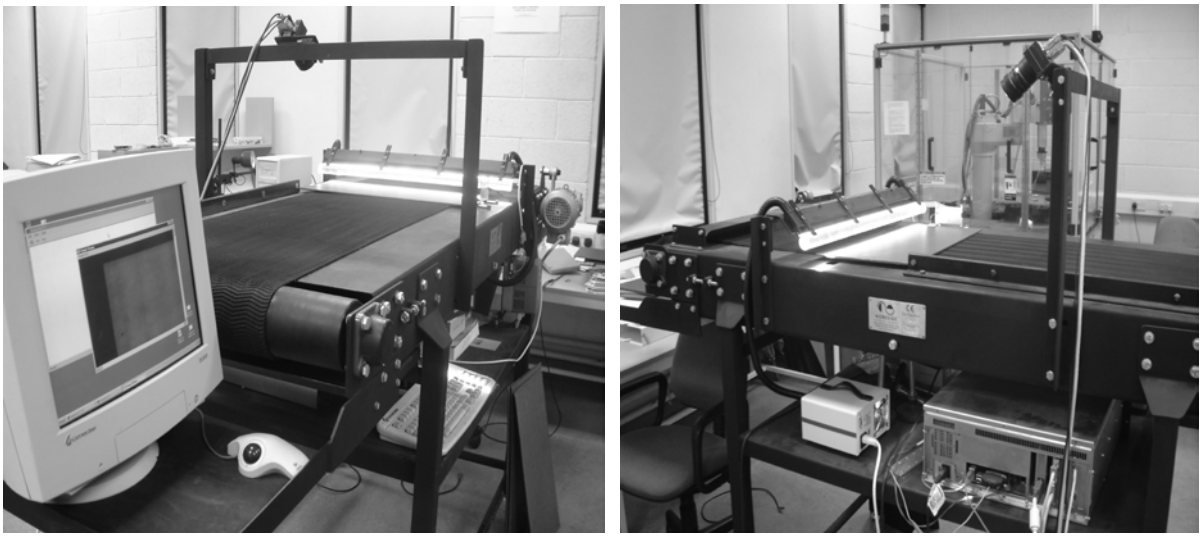

Figure 2. The prototype slate inspection system.

3.1 Illumination set-up

The illumination-set employed relies on the strong reflecting properties of the slate's surface. The light incident on the slate and the light reflected by the slate surface are equal if the quality of the slate surface is acceptable. In this regard, paint and substrate defect have reduced gloss level (except paint droplets that may have a higher gloss level than the surfaces of acceptable quality) or altered surface angles caused by lumps and depressions. This translates to a reduction in the light level arriving at the sensing device.

The inspection system described in this paper uses a collimated light source. In our experiments we have also tried an illumination set-up using a diffuse light source but the level of light reflected back to the sensing device was to low to image the slate at high resolution. A low resolution acquisition was not desirable as small defects cannot be imaged in the slate moving direction. The light level offered by the collimated light source was sufficient to image the slate at high resolution (exposure time 400μs) and for this implementation this type of illumination has been adopted. But one of the problems we encountered was the variation in depth profile across the slate due to a slight but acceptable bowing that the nominal slates

may present. The depth profile variations range from negligible to 5 mm over the slate length and up to 2 mm along the slate width. Although this does not impair slate functionality in any way, the depth profile variation raises and lowers the absolute position of the band of light relative to the camera viewing position. As a mechanical solution to force the slate into a flat position is not feasible, it was decided to widen the light stripe projected at the inspection point by defocusing the lens of the collimated light. Nonetheless, this caused a reduction in light intensity that has been compensated by using the spare capacity in the lamp controller. The width of the light stripe has been calculated using a simple trigonometric calculation and the lens was defocused such that the resulting light stripe was made equal to 25mm. This width of the light stripe made the system insensitive to depth profile uniformities of the inspected slate. The illumination light source consists of a Fostec 30" fiber optic light fitted with an adjustable cylindrical lens and two Fostec DCR III 150 W lamp controllers. It is worth noting that the solution to use collimated light has the advantage that the ambient light has negligible influence on the level of light reflected by the slate surface back to the sensing device. We had tested the inspection system under various ambient light conditions and the system proved to be insensitive to changes in the ambient lighting.

4. The inspection algorithm

The inspection algorithm comprises of a few steps. The first step involves the identification of the slate from image data to verify the presence of the nail holes. The second step involves analysing the image data in order to detect the visual defects present on the surface of the inspected slate. In the remainder of this section the steps required by the image processing procedure are detailed.

4.1 Segmentation of slate image from background and nail checking

As mentioned earlier the first step of the image processing procedure that is applied to verify if the inspected slate is defective involves the identification of slate boundaries in the image data. Slate edge detection was facilitated by cutting slots in the conveyor base and ensuring the belt width is less than that of the slate. This resulted in no light arriving back at the camera when the slate is not imaged and a sharp rise in the signal when the slate arrives at the inspection line. Thus, a simple threshold operation was sufficient to robustly identify the slate edges. Corners of the slate are located by tracking the horizontal and vertical lines to their end positions.

Once the corners of the slates are identified the next operation verifies the presence of the nail holes and if they are correctly positioned with respect to the slate boundaries. As the optical signal associated with the nail hole is significantly lower when compared to the slate surface, a threshold operation is sufficient to robustly identify them in the slate image data. The algorithm starts with identifying the nail hole placed on the left hand side of the slate. Then knowing the slate boundary (i.e. slate rotation) the algorithm verifies the presence of the remaining two nail holes situated on the right hand side of the slate. If the nail checking procedure fails the slate is classed as defective. If the nail holes are correctly positioned the algorithm fills them with pixel information adjacent to the nail hole as not to trigger visual defects when the slate is subjected to the inspection algorithm described in the next section. A graphical example illustrating the nail hole checking procedure is depicted in Figure 3.

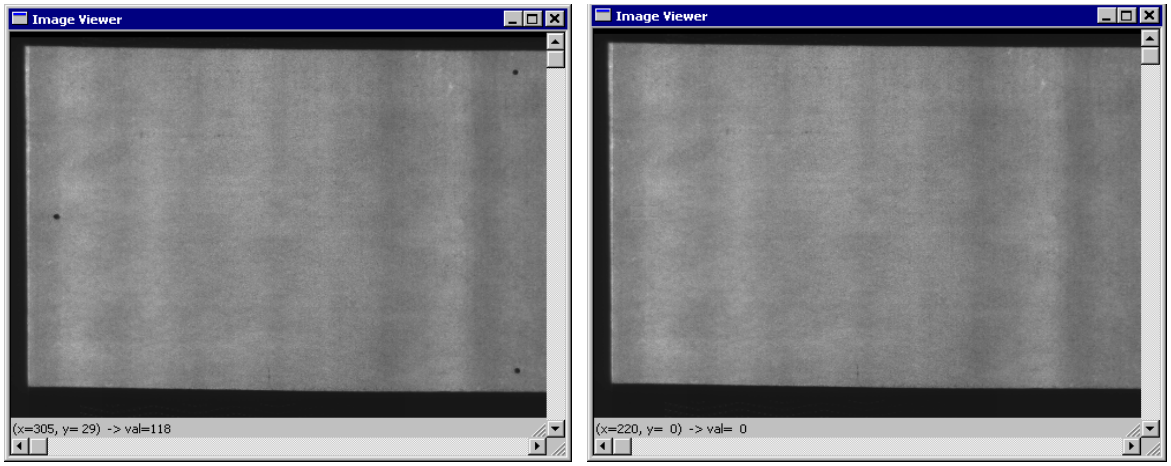

Figure 3. Nail hole checking procedure. (a) Image before nail hole inspection.
(b) Resulting image after nail hole inspection.

4.2. Texture analysis inspection

The aim of the inspection algorithm is the classification of inspected slates into two categories: defective slates and slates with acceptable quality. As mentioned in the introductory part of this paper, a number of potential algorithms can be applied to identify the visual defects present on the slate surface. Among many possible solutions the morphological and texture analysis methods look most promising. The morphological approaches appear to be more appealing to use due to their simplicity and real-time operation [4,14]. However there are a few aspects that are worth noting. The first is a relative high greyscale variation between various imaged areas of the slate. In our experiments we also found out that the mean grey level for successive slates can vary substantially (up to 20 grey levels where the average mean grey level is 167). These variations are not generated by the optical and sensing equipment but rather due to acceptable variation in slate surface color. Hence, the potential algorithm has to be able to accommodate these greyscale non-uniformities. Also it has been observed that the vast majority of defects are negligibly small relative to the whole slate image. Hence, the inspection algorithm should analyse the image data in small image sub-sections as the relative impact of the defect on the overall grey-level statistics of the section is increased [7,10]. By experimentation it has been determined that the slate image should be divided into sections of 128 ×128 pixels and the inspection algorithm should analyse them separately. The second problem is to decide which segmentation method is better suited to identify the visual defects on the slate surface. In our previous paper [4] we have advanced a multi-component morphological algorithm, where each component has been designed to be defect specific. Although the method proved to be very robust its main disadvantage is the fact that it relied on a relatively large number of threshold parameters that were experimentally determined a fact that made the algorithm difficult to be retrained if the production process would be changed.

Thus, in this paper our aim is to propose a new algorithm that is able to identify areas in the image that have similar tonal/texture characteristics. To this end it has become clear that an inspection algorithm based on texture analysis offers a higher flexibility than the morphological-based inspection algorithms. The devised inspection algorithm uses two types of distributions, namely tonal (greyscale) and texture distributions that are used as input features in a highly adaptive split and merge architecture [15]. For our implementation, Local

Binary Pattern (LBP) distributions [18] are used as texture feature while the tonal information is extracted by a self-initialising unsupervised *K-means* algorithm [5].

4.3 LBP texture feature distributions

The LBP concept developed by Ojala et al [18] attempts to decompose the texture into small texture units. A texture unit is represented in a 3×3 neighbourhood which generates 2^8 possible standard texture units. In this regard, the LBP texture unit is simply obtained by applying a simple threshold operation using the following rule:

$$E_i = \begin{cases} 0 & V_i < V_0 \\ 1 & V_i \geq V_0 \end{cases} \tag{1}$$

where V_0 is the central pixel of the 3×3 mask. The LBP is determined as follows:

$$LBP = \sum_{i=1}^{8} E_i * 2^{i-1} \tag{2}$$

As the LBP does not take into consideration the contrast of the texture which is a measure of local greyscale variation, often the LBP is used in conjunction with a contrast measure. Here, the contrast measure is the normalised difference between the greylevel of the pixels with a LBP value of 1 and the pixels with a greylevel 0 contained in the texture unit.

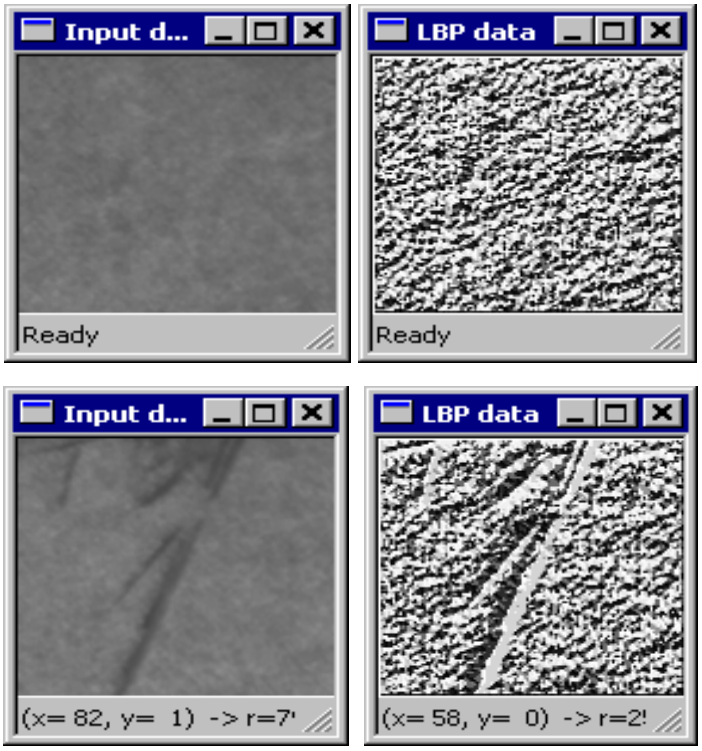

Figure 4. LBP image. (Top row) LBP image of a defect free image section. (Bottom row) LBP image for a defective image section.

The distribution of the LBP/C of the image represents the texture spectrum. The LBP/C distribution is a 2D histogram of size 256 × *b* where *b* is the number of bins for contrast measure. As suggested by Ojala et al [18] we have used 8 bins for contrast measure (our experiments confirmed that best segmentation has been achieved when 8 bins have been used to sample the contrast measure). This 2D histogram is used as a texture discriminating feature in our implementation. In Figure 4 is depicted the LBP image for a defect free and a defective image section.

4.4 Extraction of tonal features

Although the LBP/C distribution offers a good discrimination between the image areas with different characteristics, the small defects such as paint droplets, shallow shade variation and small template marks do not have a significant impact on the overall LBP/C histogram. Fortunately these defects have similar greyscale characteristics and this motivates us to use the tonal (greyscale) information as the second discriminating feature (see Figure 5).

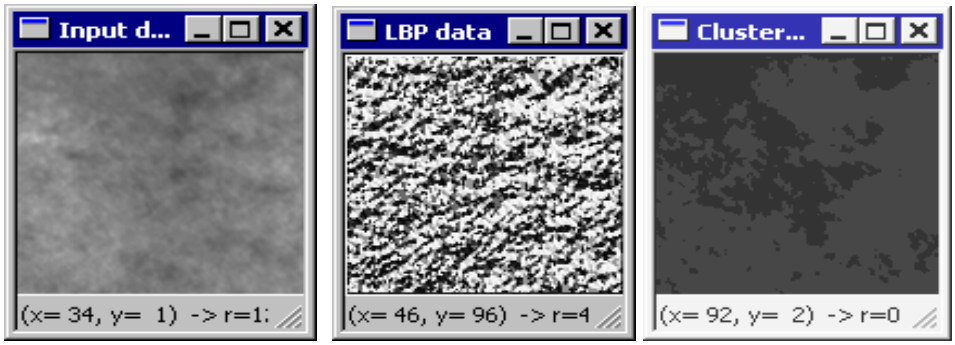

(a) (b) (c)

Figure 5. (a) Input image revealing shallow shade variation. (b) LBP data. (c) Clustered (tonal) data.

In order to extract the tonal information we have to identify the image areas with similar greyscale properties. For this purpose we have employed an unsupervised *K-means* clustering technique [5].

One problem with the standard clustering algorithms is the difficulty to input the number of clusters in the image. Also the initialisation for the *K-means* procedure is troublesome, as we do not know the information about the seeds located in the greyscale space *a priori*. To circumvent this problem we propose to identify the greyscale seeds based on a histogram analysis. To this end, the histogram has been divided uniformly into 20 regions with respect to the greyscale values and for each region the bins with the largest number of elements are identified and selected as seeds for the *K-means* procedure. As the image sections are relatively small (128 ×128) many bins of the histograms have very few elements and do not generate any seeds for the clustering algorithm. Thus if the image section is defect free, it will generate only 1-3 seeds whereas a defective regions will generate significantly more seeds for *K-means* clustering algorithm. Figure 6 depicts the images resulting after clustering for a defect free image section and for a defective image section.

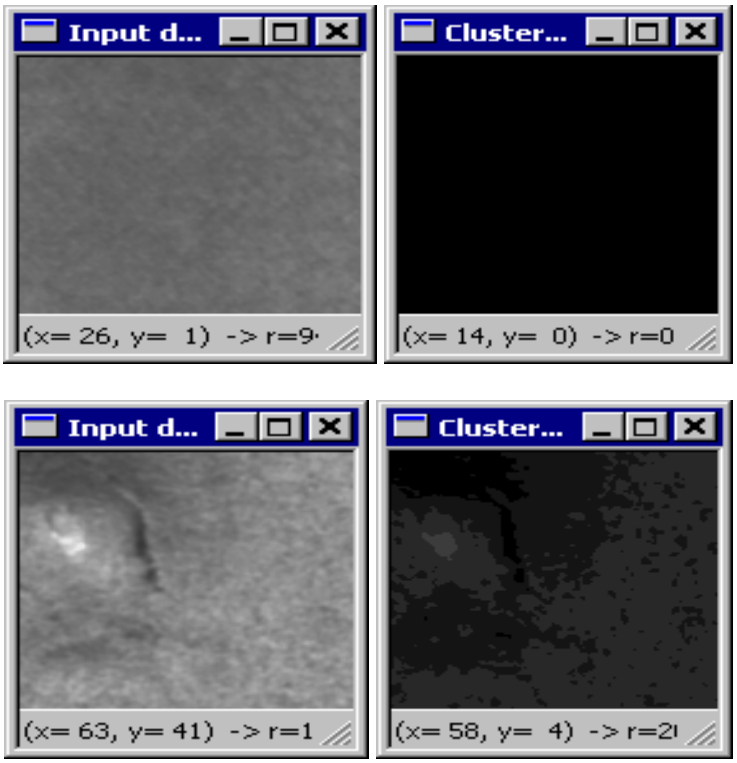

Figure 6. Clustering results. (Top row) Defect free image section.
(Bottom row) Defective (lump) image section.

4.5 Split and merge segmentation method

The segmentation method devised for the inspection algorithm is based on a split and merge computational model [15]. The first step involves recursively splitting of the image hierarchically into four sub-blocks using only the LBP/C data. In this regard, the similarity measure between the resulting 4 sub-blocks is evaluated using the *Modified Kolmogorov-Smirnov* (MKS) metric (see Appendix A). The uniformity of the region is evaluated by a decision factor as follows:

$$R = \frac{MKS_{\max}}{MKS_{\min}} > X \tag{3}$$

where MKS_{max} and MKS_{min} are the highest and lowest *MKS* values resulting after calculating the pairwise *MKS* values of the 4 sub-blocks and X is a split threshold value. The splitting process continues until the stopping rule is satisfied or the block size is smaller than a predefined value (for this implementation the minimum size for has been set to 16×16). During the splitting procedure for each block two distributions are computed, the LBP/C distribution and the distribution of labels contained in the clustered data. The splitting process is illustrated in Figure 7. Note that the splitting decision evaluates only the LBP/C *MKS* values.

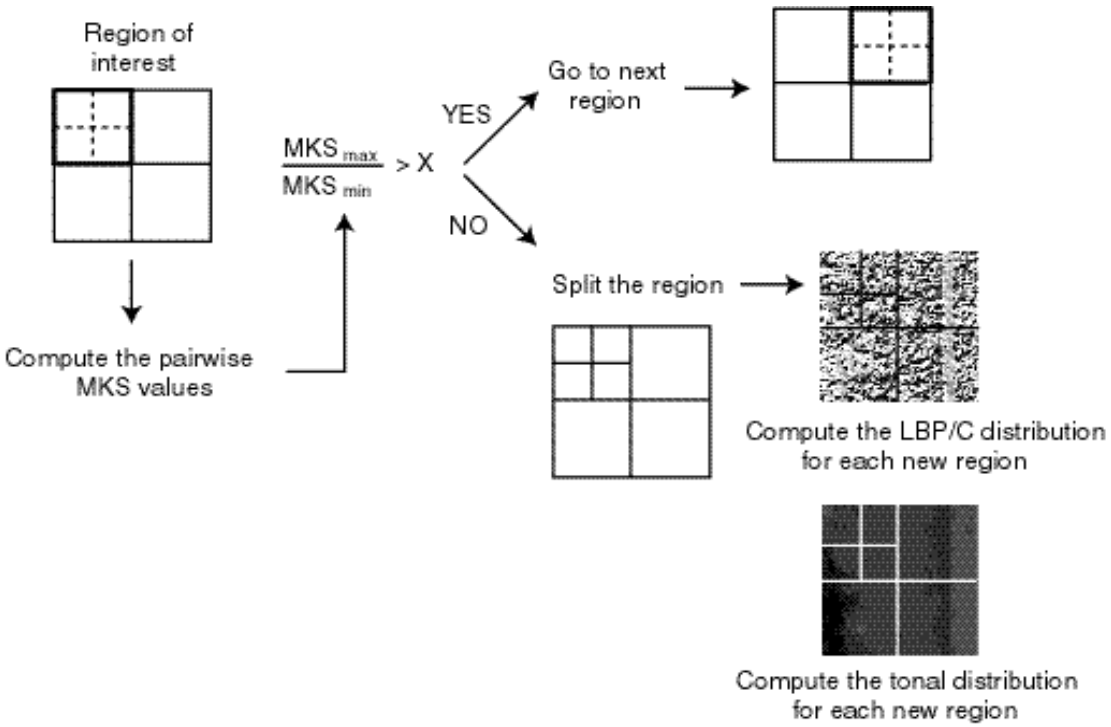

Figure 7. The splitting process.

The second step applies an agglomerative merging procedure on the image resulting after splitting in order to join the adjacent regions that have similar characteristics. This procedure calculates the *merging importance* (MI) between any adjacent regions in the split image and the adjacent regions with the smallest *MI* value are merged. The *MI* value between two adjacent regions is calculated as follows:

$$MI = w_1 * MKS_1 + w_2 * MKS_2 \tag{4}$$

where the w_1 and w_2 represent the corresponding weights for LBP/C histogram and tonal histogram respectively and the MKS_1 and MKS_2 are the *MKS* statistics for texture (LBP/C) and tonal histograms in the two adjacent regions. These adjacent regions are also referred to as the sample and model regions. In this way, the MKS similarity measures for tonal and texture distributions (histograms) implement a compound texture/greyscale image descriptor. In order to be robust this texture descriptor should be able to adapt automatically the importance of texture and greyscale (tonal) characteristics and this is assured by the values of the weights w_1 and w_2. Thus, we devise an elegant solution to determine the weights automatically by analysing a uniformity factor that is defined as the ratio between the bin with the highest number of elements in the clustered histogram and the number of pixels contained in the whole distribution. This uniformity factor is evaluated for the two adjacent regions under consideration as follows:

$$k_j = \max\left\{\frac{Clust[i]}{N_p}\right\} \quad , \; k_j \le 1 \tag{5}$$

where *Clust* defines the tonal histogram of the region *j*, *i* is the bin index and N_p represents the number of pixels in the region *j* that is evaluated.

The uniformity factor is calculated for sample and model regions (k_1 and k_2). If the difference between k_1 and k_2 is less than 0.1 then we can assume that the sample and model regions have a similar uniformity factor and the tonal information should have a higher importance. Thus, the weight values are assigned as follows: $w_2 = (k_1 + k_2)/2$ (tonal) and $w_1 = 1 - w_2$ (texture). If the difference between k_1 and k_2 is high this indicates that the regions are not uniform and the algorithm gives similar weights for texture and tonal statistic, i.e. $w_1 = w_2 = 0.5$.

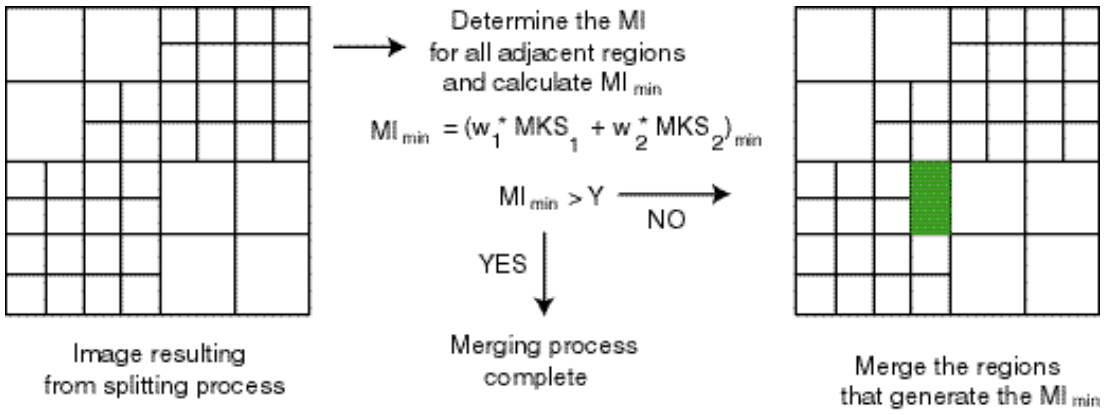

Figure 8. The merging process.

The agglomerative merging procedure is repeated iteratively until the minimal *merging importance* (MI) value between all adjacent regions is higher than a threshold value, i.e. *Min(MI) > Y*. The merging process operations are illustrated in Figure 8 and a graphical example is illustrated in Figure 9.

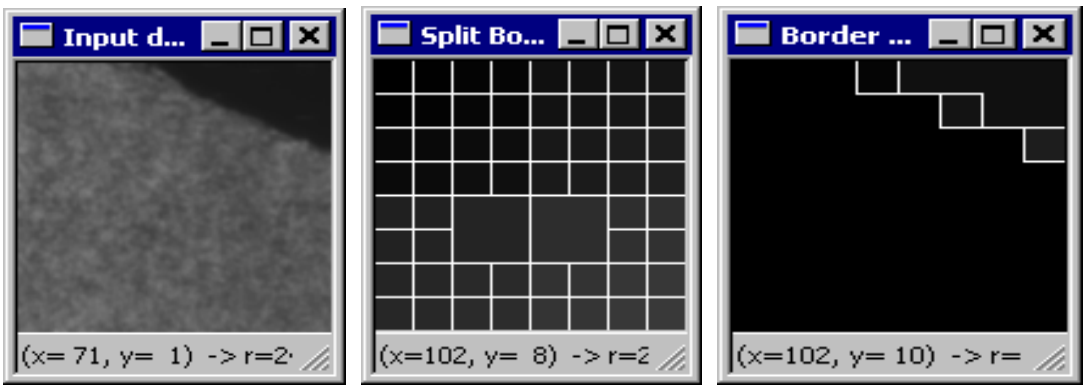

(a) (b) (c)

Figure 9. Image segmentation process. (a) Input defective section. (b) Image resulting after splitting. (c) Image resulting after merging.

Once the merging process is complete the resulting regions contained in the segmented image (see Figure 8c) are analysed in order to verify if they belong to a defective area. For this purpose we have devised a simple test routine. If the segmented data has only one region the inspection algorithm verifies if the slate section is painted. This involves a very simplistic test by verifying if the greylevel mean is above 100. If the greylevel mean of the image section is lower than 100 the image section is defective, otherwise it is classed as acceptable.

If the segmented data has more than one segmented region then several tests are performed in order to verify if the section is defective or not. The visual defects can be roughly classed in template marks and shade variations. The paint defects (efflorescence and shade variation) can be identified by checking the variation in the greyscale values whereas the template marks (lumps and bad slate formation) presence is verified by a simple count of the edge pixels contained in the segmented region under evaluation (for computational purposes we have used for this task the Sobel edge detector [21]). The first test (check for the presence of paint defects) verifies if the greylevel means of the segmented regions are above 100 (slate painted) and the inter-region variation is smaller than 20 grey levels. If the difference of the mean greylevel of two segmented regions is higher than 20 grey levels or the mean greylevel of any region is smaller than 100 the section is classed defective. If this test is passed the regions are tested in order to verify if substrate defects are present. For this purpose the edge data returned by the Sobel edge detector is evaluated and the number of edge pixels in each segmented region is counted. If the number of edge pixels is higher than 10% of the total number of pixels in the region then a substrate defect is present and the image section is classed as defective. Otherwise the image is classed as acceptable.

These tests were necessary, as small scratches and mild shade variations are often present on slates that are considered to have an acceptable surface finish (see Figure 3b-all slate image and Figure 10-slate subsections). The aim of these tests was to eliminate the false positive decisions caused by under segmentation.

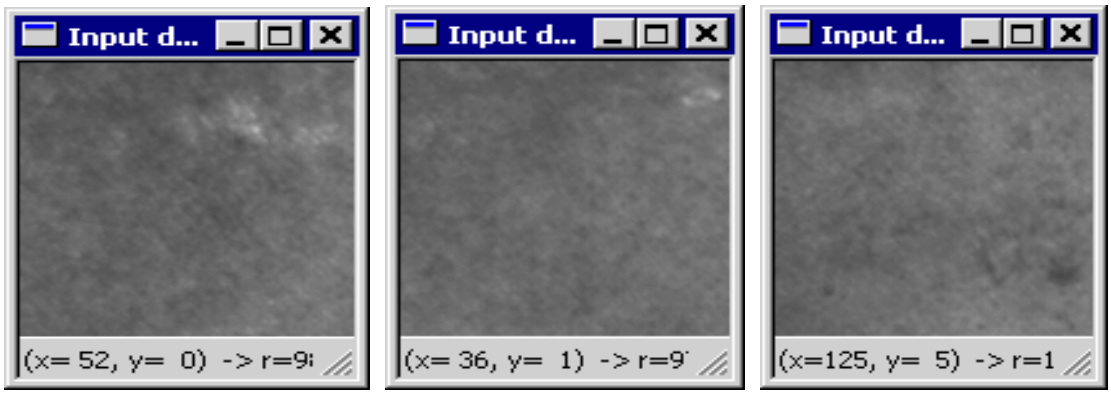

Figure 10. Image sections with acceptable finish but presenting a small but acceptable shade variation.

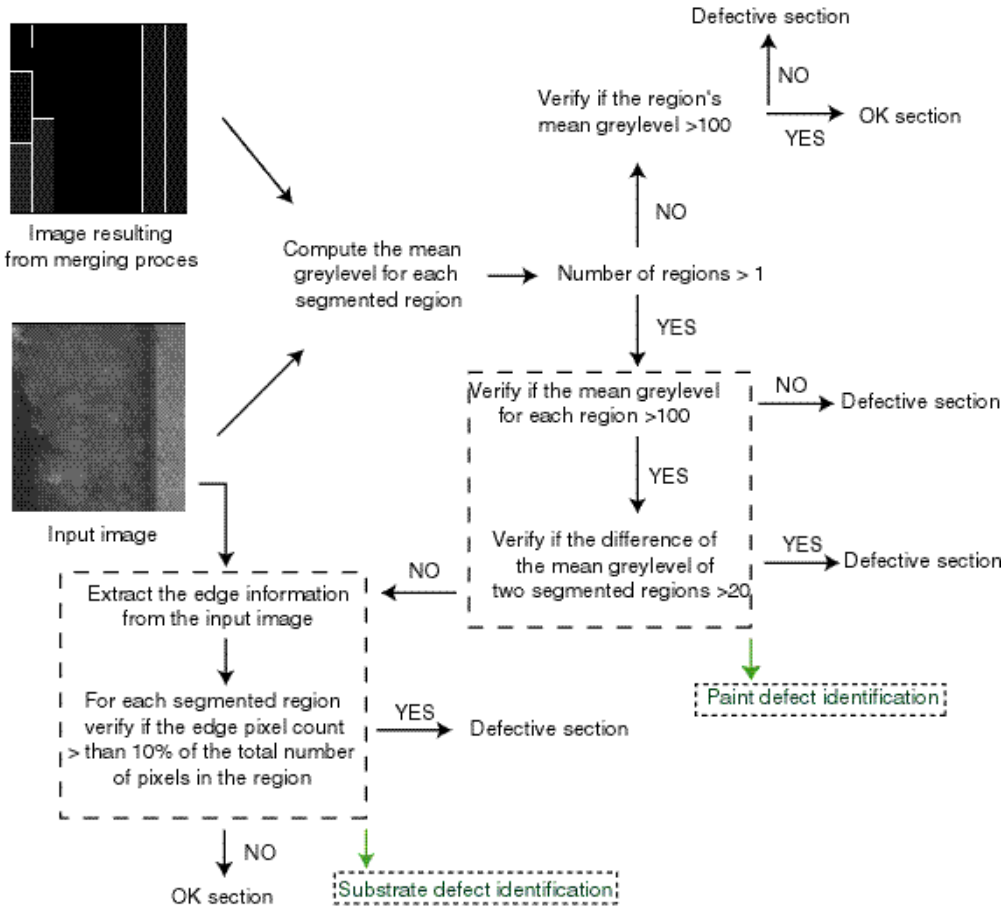

Figure 11. The operations required by the inspection algorithm.

5. Experiments and results

The conveyor speed was set to 38m/min and the camera exposure was set to 400μs giving a scan frequency of 2.5KHz. For this scan frequency the cross direction resolution is 0.221mm and the moving direction resolution is 0.244mm. The variability of the conveyor speed has been measured by imaging the same slate several times and this process is repeated for 16 test slates with known image dimensions. The measurements for a test slate that is repeatedly imaged for 10 times ranged from 298.3 to 300.7, while the measurements for 16 slates ranged from 295.9 to 300.7 mm (a small variation (less than 1mm) in size from slate-to-slate was observed). The conveyor speed variations slightly effects the actual image resolution in the moving direction but the resolution change is very small (approx. 0.8%) and does not have any negative effect on the inspection results.

The inspection algorithm has been designed to have as few threshold parameters as possible and currently only two parameters for split and merge algorithm had to be set experimentally. The threshold parameter for splitting has been set to 1.1 in order to achieve a slight over-splitting in order to prevent the situations when a small defect is divided by two adjacent regions (remember that the splitting process evaluates only the LBP/C (texture) data). The threshold parameter for merging has been set to 0.75 and it has been trained on best defect-free slates in order to obtain a single segmented region resulting from the merging process.

For other slates (reference or defective) the segmented data resulting from the merging process will have more than one region and each image section is evaluated for visual defects using the procedure illustrated in Figure 11.

The inspection system has been tested on 235 slates (112 reference-defect free slates and 123 defective slates) and the success rate for correct identification of acceptable slate was 98.12 % for defect free slates and 99.18% for defective slates. The classification of defective slates and defect-free slates was performed by an experienced operator based on a visual examination. A detailed performance characterisation of the inspection system is depicted in Table 2.

Slate type	Quantity	Fail	Pass	Accuracy
Reference	112	2	110	98.21 %
Defective	123	123	0	100 %
Total	235			99.14 %

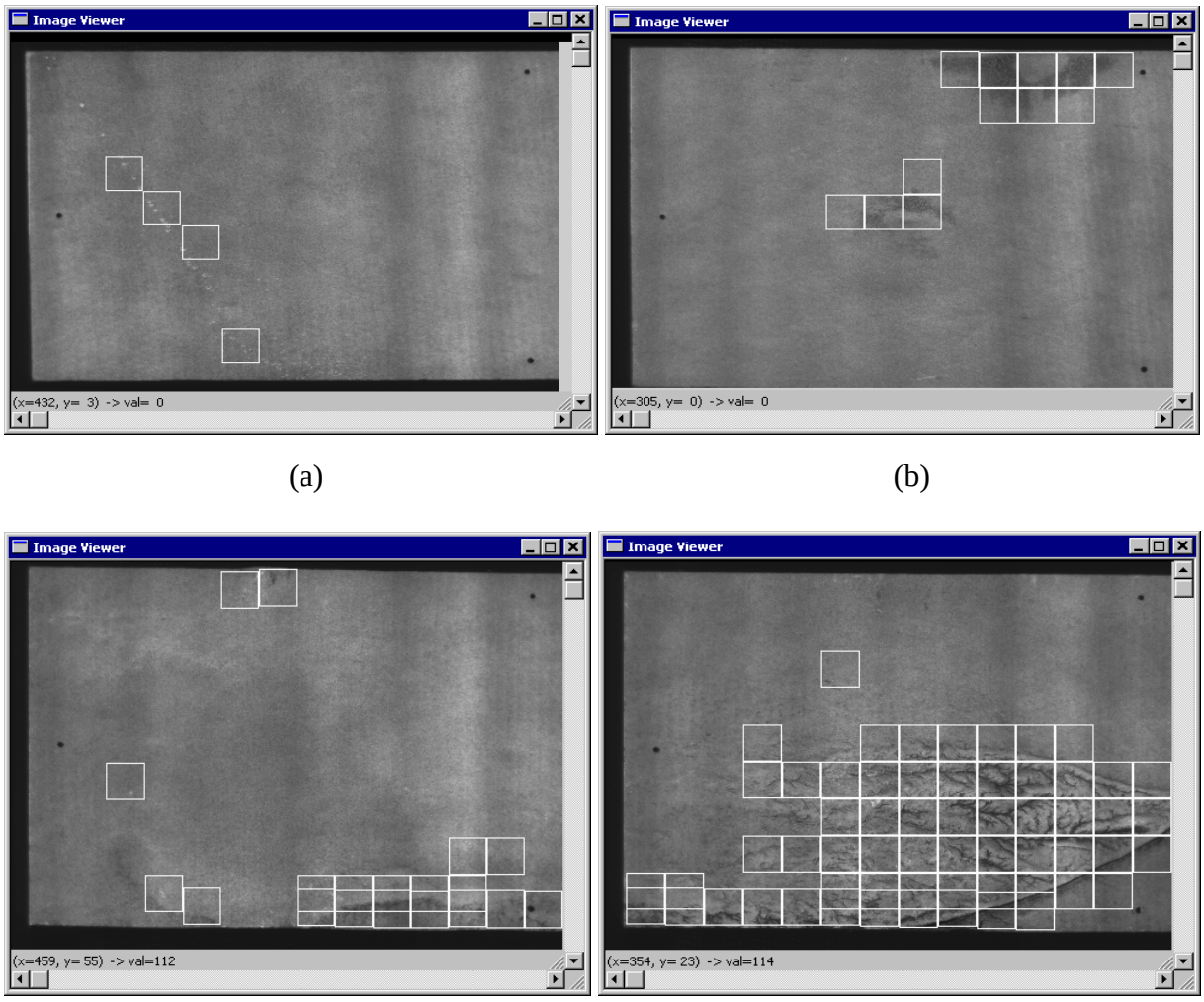

(a) (b)

(c) (d)

Figure 12. Visual defects identification on representative slates (defective image sections marked with a white box). (a and b) Paint defects. (c and d) Substrate defects

The defective slates used in our experiments contained a large range of paint and substrate defects and the efficiency of the system with respect to rejecting defective slates is 100%. The reference slates were classified as slates of acceptable quality with an accuracy of 98.21 %. Two slates were classified as defective slates. These slates were classed as defective due to the detection of the wax marks. The wax mark contamination may be produced during handling and transportation and may not be present when the slates are inspected on the production line. These results give an overall inspection accuracy of 99.14% with respect to correct classification for reference and defective slates. Figure 12 illustrates the identification of visual defects (paint and substrate) on several representative defective slates.

6. Conclusions

The experimental data indicates that automating the inspection of painted slates can be achieved and the installation in a factory is a realistic target. The devised inspection prototype has been tested in a factory-style environment and these tests were an important part of the development process. The development of a robust slate inspection system was challenging, as we have to provide adequate solutions for each part of the system including the illumination and image acquisition set-up, conveying requirements and equally important the image processing inspection algorithm. In this regard, we proposed an illumination set-up that is able to minimise the negative effects generated by the slate depth variation and the mechanical vibrations caused by the conveying system. The major part of the system was the development of a robust inspection algorithm that is able to identify the visual faults on the slate surface. To address this issue, in this paper we proposed an adaptive texture analysis scheme that was able to accommodate the acceptable local variation in the slate image data but at the same time the inspection algorithm is able to robustly identify the visual defects present on the slates surface. The overall performance of the slate inspection system indicates that the proposed integrated solution presented in this paper can be considered as a replacement for the manual inspection system that is currently employed to grade the quality of slates.

Acknowledgments

This research work was financed by Enterprise Ireland.

References

[1] Boukouvalas C., De Natale F., De Toni G., Marik R., Mirmehdi M., Petrou M., Le Roy P., Salgari R., and Vernazza F., “An integrated system for quality inspection of tiles”, *Proc. International Conference on Quality Control by Artificial Vision OCAV’97*, Toulouse, France, pp. 49-54, 1997.

[2] Boukouvalas C. Kittler J., Marik R. and Petrou M., “Colour grading of randomly textured ceramic tiles using colour histograms”, *IEEE Transactions on Industrial Electronics*, 46(1), pp. 219-226, 1999.

[3] Batchelor B.G. and Waltz F.M., *Intelligent Machine Vision: Techniques Implementations and Applications*, Springer Verlag, ISBN: 3-540-76224-8, 2001.

[4] Carew T., Ghita O. and Whelan P.F., A vision system for detecting surface faults on painted slates, *Mechatronics 2002, The 8th Mechatronics Forum International Conference*, University of Twente, Enschede, Netherlands, 2002.
[5] Duda R.O, Hart P.E. and Stork D.G., *Pattern Classification*, Wiley, 2nd Edition, ISBN: 0-471-05669-3, 2001.
[6] Fernandez C., Fernandez J. and Aracil R., "Integral on-line machine vision inspection in the manufacturing process of ceramic tiles", *Proc of SPIE*, vol. 3306, 1998.
[7] Fioravanti S., Fioravanti R., De Natale F., Marik R., Mirmehdi M., Kittler J. and Petrou M., "Spectral rank order approaches to texture analysis", *European Transactions on Communications*, 6(3), pp. 287-300, 1995.
[8] Kukkonen S., Kälviäinen H., and Parkkinen J., "Color features for quality control in ceramic tile industry", *Optical Engineering*, 40(2), pp. 170-177, 2001.
[9] Kyllönen J. and Pietikäinen M., "Visual inspection of parquet slabs by combining color and texture", *Proc. IAPR Workshop on Machine Vision Applications (MVA'00)*, Tokyo, Japan, 187-192, 2000.
[10] Latif-Amet A., Ertüzün A. and Erçi A, "An efficient method for texture defect detection: sub-band domain co-occurrence matrices", Image and Vision Computing, 18(6-7), pp.543-553, 2000.
[11] Mäenpää T, Viertola J. and Pietikäinen M., "Optimising colour and texture features for real-time visual inspection", *Pattern Analysis and Applications*, 6(3):169-175, 2003.
[12] Muller S. and Nickolay B., "Morphological image processing for the recognition of surface defects", *Proc. of SPIE*, vol. 2249, pp. 298-307, 1994.
[13] Newman T. and Jain A., "A survey of automated visual inspection", *Computer Vision and Image Understanding*, 61(2), pp.231-262, 1995.
[14] Nieniewski M., Chmielewski L., Jóźwik A. and Sklodowski M, "Morphological detection and feature-based classification of cracked regions in ferrites", *Machine Graphics and Vision*, 8(4), pp. 699-712, 1999.
[15] Padmapriya N., Ghita O. and Whelan P.F., "Integration of Feature Distributions for Colour Texture Segmentation", *ICPR2004 - 17th International Conference on Pattern Recognition*, Cambridge, UK, pp. 716-719, 2004.
[16] Patek D., Goodard J., Karnowski T., Lamond D. and Hawkins T., "Rule based inspection of printed green ceramic tape", *International Society for Optical Engineering, Photonics West Symposium on Electronic Imaging*, pp.22-30, 1998.
[17] Peñaranda J., Briones L. and Florez J., "Colour machine vision system for process control in ceramic industry", *Proc of SPIE*, vol. 3101, pp. 182-192, 1997.
[18] Ojala T., Pietikainen M. and Harwood D., "A comparative study of texture measures based on feature distributions", *Pattern Recognition*, 29(1), pp. 51-59, 1996.
[19] Smith M.L. and Stamp R.J., "The automatic visual inspection of textured ceramic tiles", *Computers in Industry*, 43(1), pp. 73-82, 2000.
[20] Tobias O., Seara R., Soares F and Bermudez J., "Automated visual inspection using the co-occurrence approach", *IEEE Midwest Symposium on Circuits and Systems*, pp. 154-157, 1995.
[21] Whelan P.F. and Molloy D., *Machine Vision Algorithms in Java, Techniques and Implementation*, Springer (London), ISBN: 1-85233-218-2, 2000.

Appendix A - Modified Kolmogorov-Smirnov statistic

The *Modified Kolmogorov-Smirnov* (MKS) statistic is a non-parametric test that is used to compare two independent distributions. The *MKS* similarity measure is defined as the sum of the absolute value of the discrepancies between the normalised cumulative sample distributions (i.e. the number of pixels contained in each bin is divided by the total number of pixels contained in the distribution). The *MKS* statistic is calculated as follows:

$$D(s,m) = \sum_{i=0}^{n} \left| \frac{F_s(i)}{n_s} - \frac{F_m(i)}{n_m} \right| \tag{1a}$$

where n represents the number of bins of the sample and model distributions (histograms), n_s and n_m are the number of pixels of the sample and model distributions and $F_s(i)$ and $F_m(i)$ represent the number of pixels contained by the bin with index i of the sample and model distributions respectively. The *MKS* similarity measure is normalised, hence its result is bounded, and this is a significant advantage over other statistical measures such as *G statistic* or *Chi square test* especially when the similarity test is applied to sparsely populated distributions.